

Evolution of Strategies to Prepare Synthetic Mimics of Carboxylate-Bridged Diiron Protein Active Sites

*Loi H. Do, Stephen J. Lippard**

Department of Chemistry, Massachusetts Institute of Technology, Cambridge, MA 02139.
U.S.A.

*To whom correspondence should be addressed: lippard@mit.edu.
Department of Chemistry, Room 18-498
Massachusetts Institute of Technology
77 Massachusetts Avenue
Cambridge, MA 02139-4307
Phone: (617) 253-1892, Fax: (617) 258-8150

Abstract

We present a comprehensive review of research conducted in our laboratory in pursuit of the long-term goal of reproducing the structures and reactivity of carboxylate-bridged diiron centers used in biology to activate dioxygen for the conversion of hydrocarbons to alcohols and related products. This article describes the evolution of strategies devised to achieve these goals and illustrates the challenges in getting there. Particular emphasis is placed on controlling the geometry and coordination environment of the diiron core, preventing formation of polynuclear iron clusters, maintaining the structural integrity of model complexes during reactions with dioxygen, and tuning the ligand framework to stabilize desired oxygenated diiron species. Studies of the various model systems have improved our understanding of the electronic and physical characteristics of carboxylate-bridged diiron units and their reactivity toward molecular oxygen and organic moieties. The principles and lessons that have emerged from these

investigations will guide future efforts to develop more sophisticated diiron protein model complexes.

Keywords: carboxylate-bridged diiron modeling, dioxygen activation, biomimetic chemistry, ligand design

1. Introduction

Understanding the role of metal ions in dictating protein structure and function is a central theme in bioinorganic research [1-4]. In addition to the arsenal of modern physical techniques and instrumentation available for studies of biomolecules [5], synthetic modeling has been pursued as a complementary method for understanding complex biological systems [6]. It provides a convenient simplification of elaborate macromolecules in a real, rather than a virtual, computational, platform [7]. By reducing a metalloprotein to its functional core, it is possible to learn the extent to which the chemistry that occurs at the metal center is predominantly a result of the inorganic component or a consequence of the protein complex as a whole. Synthetic modeling also provides an opportunity to access chemistry that has not yet been achieved using simple biological building blocks under ambient conditions. Some of the most remarkable transformations in nature, such as nitrogen fixation [8-11], water splitting [12], and hydrogen production [13], are performed by metalloenzymes under physiological conditions. Reproducing such chemical reactivity in an efficient manner has the potential not only to revolutionize the chemical industry but also to provide new sustainable sources of energy [14]. Finally, the synthetic challenges of modeling chemistry will push the limits of current synthetic methodology. Although natural product synthesis has been largely aided by an understanding of organic chemistry [15], inorganic synthesis is not governed by the same set of well-defined rules

[16]. Nature works at a kilohertz and requires, in many cases, first-row transition metals as active sites for catalysis. Controlling the kinetic stability and resultant nuclearity of metal centers using organic ligands comprises the single significant challenge in bioinorganic modeling chemistry.

Small-molecule metalloprotein mimics are prepared using one of two design strategies [4]. The *biomimetic* approach seeks to duplicate the active site structure as faithfully as possible, particularly in matching the identity and geometric arrangement of ligands in the primary coordination sphere. The *bio-inspired* approach, on the other hand, only requires that the synthetic model shares some common features with those of the protein core, unrestricted by the type or position of ligands coordinated to the metal center. For modeling studies, the former is preferred over the latter because biomimetic complexes more accurately reproduce the characteristics of the biological center under investigation.

1.1. Carboxylate-Bridged Diiron Proteins

Carboxylate-bridged diiron proteins are involved in essential physiological processes [17, 18]. Although their roles vary, the first step in their respective reaction mechanisms involves binding and activation of dioxygen. In hemerythrin (Hr) [19], the O₂ molecule coordinates to a single iron site and acquires two electrons and a proton to generate a (hydroperoxo)diiron(III) unit (Scheme 1, top). This process is reversible and is the basis for O₂ transport in some marine invertebrates. Unlike hemerythrin, ribonucleotide reductase (RNR) [20] and bacterial multi-component monooxygenases (BMMs) [21] consume dioxygen to perform catalytic reactions (Scheme 1, middle and bottom, respectively). Activation of O₂ by these enzymes leads to formation of (peroxo)diiron(III) or di(μ -oxo)diiron(IV) complexes that are capable of oxidizing organic moieties [22-26]. The high-valent diiron intermediate in the R2 subunit of RNR

generates a tyrosyl radical that ultimately initiates the first step in DNA biosynthesis, conversion of ribo- to deoxyribonucleotides, whereas that in the hydroxylase component of the BMMs is responsible for inserting an oxygen atom into the C–H bond of hydrocarbon substrates. The most well-studied member of the BMM family is soluble methane monooxygenase (sMMO) [27], which is unique for its ability to hydroxylate methane to methanol. Recent studies have revealed that other classes of enzymes containing carboxylate-bridged diiron motifs also exist in biology [28-30].

These diiron proteins contain two iron atoms that are coordinated by imidazole and carboxylate residues, where at least one of the carboxylate groups bridges the two metal centers [17]. The structural similarities between the active sites of this protein family indicate that their functional differences are derived from variations in their Asp/Glu/His amino acid combinations and/or careful tuning of their tertiary and quaternary protein structures. Discerning factors that may contribute to their mechanism of action is an important goal in synthetic model studies [31, 32].

The following is a chronological account of the strategies and tactics employed in our laboratory to prepare structural and functional mimics of diiron protein active sites. This work has evolved a rational basis for ligand design based on the findings that resulted from studies of the various model systems. The reader is referred elsewhere for more general reviews of synthetic modeling of carboxylate-bridged diiron proteins [31-36].

2. Ligand Platforms

2.1. Mononucleating, Polydentate *N*-Heterocyclic Ligands

The first successful attempt to prepare a mimic of the diiron core in Hr was achieved using hydrotris(pyrazolyl)borate (TP⁻) (Table 1) [37, 38], a tripodal ligand widely employed in transition metal chemistry. Reaction of TP⁻, iron(III), and acetate led to the spontaneous self-assembly of [Fe^{III}₂(μ-O)(μ-CH₃CO₂)₂(TP)₂] (**1**), the structure of which closely matches that of metHr, the inactive form of Hr [19]. Reaction of **1** with an H⁺ donor led to formation of [Fe^{III}₂(μ-OH)(μ-CH₃CO₂)₂(TP)₂]⁺ (**2**), a stable protonated analogue of **1** [39]. Spectroscopic and magnetic measurements of the (μ-oxo)di(μ-carboxylato)diiron(III) and (μ-hydroxo)di(μ-carboxylato)diiron(III) compounds provided valuable benchmarks for identifying such units in biology [40, 41]. When **1** was exposed to H₂¹⁸O, the ¹⁶O bridge was readily exchanged for ¹⁸O, indicating that of the inability to exchange water into the protein is due to inaccessibility of H₂O to the diiron core rather than an intrinsic property of the {Fe^{III}₂O}⁴⁺ unit. An undesirable feature of **1** and **2** is that the facially capping nature of the TP⁻ ligands does not allow for open coordination sites, which are required for O₂ binding. Moreover, reduction of the diiron(III) species resulted in irreversible dissociation to monoiron complexes [38].

To access the asymmetric diiron center in Hr, the denticity of the capping ligand was reduced from three to two by using bis(1-methylimidazol-2-yl)phenylmethoxymethane (BIPhMe) (Table 1) [42, 43]. Stirring iron(II) formate with BIPhMe in methanol provided [Fe^{II}₂(μ-HCO₂)₃(HCO₂)(BIPhMe)₂] (**3**). X-ray crystallography revealed a dinuclear structure with both five- and six-coordinate iron sites, in which each metal ion is bound by a BIPhMe ligand and bridged by three formate groups. A terminal acetate group completes the coordination sphere of the six-coordinate iron atom. Complex **3** reacts instantaneously with dioxygen to give [Fe^{III}₂(μ-O)(μ-HCO₂)₂(HCO₂)₂(BIPhMe)₂] (**4**), with no detectable intermediates. Manometric measurements indicated that 0.5 equiv of O₂ are consumed per

diiron(II) complex, suggesting that **4** is formed via a tetranuclear dioxygen species. The behavior of **3** toward dioxygen is different from that of deoxyHr, however, which binds O₂ reversibly (Scheme 1, top) [19].

2.2. Dicarboxylate Ligands

To increase the structural integrity of the carboxylate-bridged diiron center, several dicarboxylate ligands were explored as dinucleating platforms. The first of these, *m*-phenylenedipropionate (MPDP²⁻, Table 1) [44, 45], was selected because the distance between its β -methylene carbon atoms matches the 6 Å separation between acetate methyl carbon atoms in [Fe^{III}₂(μ -O)(μ -CH₃CO₂)₂(TP)₂] (**1**) [37]. The use of MPDP²⁻ facilitated the synthesis of [Fe^{III}₂(μ -O)(MPDP)(bpy)₂Cl₂] (**5**) (bpy = 2,2'-bipyridine) and [Fe^{III}₂(μ -O)(MPDP)(BIPhMe)₂Cl₂] (**6**, Table 1), complexes that could not be obtained from self-assembly using two equivalents of simple monocarboxylate anions. The cyclic voltammogram of [Fe^{III}₂(μ -O)(MPDP)(TP)₂] (**7**), an analogue of **1**, showed that mononuclear [Fe^{II}(TP)₂] and [Fe^{III}(TP)₂]⁺ species are generated upon electrochemical reduction and oxidation, respectively. Thus, linking the carboxylate groups using MPDP²⁻ does not impart the desired additional stability.

To obtain a more robust bridging framework, *m*-xylenediamine bis(Kemp's triacid)imide (XDK²⁻, Table 1), a compound devised for molecular recognition in organic chemistry [46, 47], was employed. The rigid conformation of the carboxylate units in XDK²⁻ provides a well-defined cleft for assembly of homo- and heterodimetallic complexes [48-51]. A diiron(III) compound, [Fe^{III}₂(μ -O)(XDK)(CH₃OH)₅(H₂O)](NO₃)₂ (**8**), was readily prepared from iron(III) nitrate and XDK²⁻ [52]. Kinetic studies of the substitution of coordinated solvents in **8** by either 2,2'-bipyridine or *N*-methylimidazole suggested that anion binding and exchange at the active site of hemerythrin proceed with rates similar to those exhibited by small-molecules and that the

protein scaffold does not alter the intrinsic rate of terminal ligand exchange at the diiron center. Preparation of a series of pseudohalide-bound diiron(III) compounds of the formula $[\text{Fe}^{\text{III}}_2(\mu\text{-O})(\text{XDK})(\text{bpy})_2(\text{X})_2]$, where $\text{X} = \text{NCS}^-$, NCSe^- , or N_3^- , facilitated detailed studies of the spectroscopic signatures of molecules with terminal ligation to carboxylate-bridged diiron units [53]. A notable discovery was the appearance of only one asymmetric $^{15}\text{NNN}^-$ stretch in the azide derivative; apparently this spectroscopic feature is not sufficient to discount the possibility of a terminally coordinated azide group because isotopically shifted peaks may be too close to one another in energy to be resolved.

The XDK^{2-} ligand also supports carboxylate-bridged diiron(II) units having the general composition $[\text{Fe}^{\text{II}}_2(\text{XDK})(\mu\text{-RCO}_2)(\text{RCO}_2)(\text{N-donor})_2]$, where $\text{R} = t\text{-Bu-}$ (pivalate), PhCy- (1-phenylcyclohexylcarboxylate), Ph- (benzoate), $i\text{Pr-}$ (isobutyrate), or $t\text{BuCH}_2\text{-}$ (1-*tert*-butylacetate); $\text{N-donor} = \text{py}$ (pyridine), 3-Fpy (3-fluoropyridine), N-MeIm (*N*-methylimidazole), or $\text{N-}t\text{BuIm}$ (*N-tert*-butylimidazole) [54-56]. More sterically hindered XDK^{2-} variants, containing either propyl (PXDK^{2-}) or benzyl (BXDK^{2-}) in place of methyl substituents on the Kemp's triacid moiety, could also be employed to assemble similar diiron(II) compounds. The asymmetric bridging mode of the ancillary carboxylate to the diiron(II) core is determined by both steric and electronic factors [56]. X-ray structural studies suggested that greater steric repulsion between XDK^{2-} and the external carboxylate, and more basic N-donors , favor a *syn,syn*-bidentate bridging mode of the ancillary carboxylate rather than a *syn,anti*-monodentate one. For complexes having sufficiently bulky groups, such as $[\text{Fe}^{\text{II}}_2(\text{XDK})(\mu\text{-PhCyCO}_2)(\text{PhCyCO}_2)(\text{py})_2]$ (**9**, Table 1), exposure to O_2 led to formation of stable peroxo adducts at low temperature [56]. Although these (peroxo)diiron(III) species could not be crystallized for X-ray diffraction studies, resonance Raman measurements indicated that the

dioxygen molecule is bound in a μ -1,2 fashion. Reactivity studies of the $\{\text{Fe}^{\text{III}}_2(\text{O}_2)\}^{4+}$ units revealed that they are nucleophilic [57], rather than electrophilic like the oxygenated intermediates in the BMMs [58, 59]. When warmed above -65°C , the $\{\text{Fe}^{\text{III}}_2(\text{O}_2)\}^{4+}$ species rapidly decayed, initiating a radical chain pathway that oxidized solvents with weak to intermediate C–H bond strengths. Despite having the same ligand stoichiometry as that of the (peroxo)diiron(III) species in sMMOH (H_{peroxo}) and related enzymes [27], the synthetic analogues do not reproduce the substrate scope, product selectivity, and probably the reaction mechanism of the diiron monooxygenases. It is possible that the doubly bridging XDK^{2-} ligand in the synthetic models is too rigid to allow an H_{peroxo} -like structure to be generated, a likely prerequisite for attaining the high oxidizing power of the diiron protein oxygenated intermediates.

A continued search for a ligand that is sufficiently pre-organized yet structurally flexible led to examination of other dicarboxylate motifs. One potential candidate is the dibenzofuran-4,6-bis(diphenylacetate) dianion ($\text{Ph}_4\text{DBA}^{2-}$, Table 1) [60, 61]. As in XDK^{2-} , $\text{Ph}_4\text{DBA}^{2-}$ has two orthogonal carboxylate groups that can support an $\{\text{Fe}^{\text{III}}_2\text{O}\}^{4+}$ core. The $\text{Ph}_4\text{DBA}^{2-}$ ligand, however, has more conformational freedom than XDK^{2-} because the C–C bonds linking the carboxylate groups to the dibenzofuran unit can rotate freely. The compound $[\text{Fe}^{\text{II}}_2(\mu\text{-OH})(\text{Ph}_4\text{DBA})(\text{TMEDA})_2(\text{CH}_3\text{CN})]^{+}$ (**10**, Table 1), where $\text{TMEDA} = N,N,N',N'$ -tetramethylethylenediamine, was prepared from $\text{Ph}_4\text{DBA}^{2-}$, triethylamine, TMEDA, and iron(II) triflate. The structure of **10** is unique because it is the first synthetic complex to reproduce the (μ -hydroxo)di(μ -carboxylato)diiron(II) core of deoxyHr [19], having an open coordination site for binding of a terminal ligand. When **10** was treated with dioxygen at -78°C in the presence of 3 equiv of *N*-MeIm in CH_2Cl_2 or in neat EtCN, a red-orange species (**11**) appeared that decayed

after ~10 min. The UV-visible (UV-vis), Mössbauer, resonance Raman, and EXAFS spectra of the transient intermediate closely match those of oxyHr (Scheme 1, top), strongly suggesting that **11** contains a (hydroperoxo)(μ -oxo)diiron(III) unit. Unlike Hr, however, oxygenation of **10** is irreversible and leads to decomposition to form a tetrairon(III) cluster.

A fourth dicarboxylate ligand, α,α -5,15-bis(α -*N*-(Kemp's triacid imido)-*o*-tolyl)-2,8,12,18-tetraethyl-3,7,13,17-tetramethylporphyrin (PDK⁴⁻, Table 1), was prepared by replacing the *m*-xylenediamine linker of XDK²⁻ with a porphyrin unit [62]. The construct was designed such that activation of O₂ within a trimetallic cavity would offer the possibility of supplying additional electrons to the carboxylate-bridged diiron centers, much like the reductase component of sMMO [27]. A triiron(II) compound, [Fe^{II}₃(PDK)(Lut)(Br)₂(HBr)] (**12**, where Lut = 2,6-lutidine, Table 1), was successfully prepared following metallation with iron(II) bromide [63]. When iron(II) chloride was used instead of iron(II) bromide in the preparation, a mixed-valent heptairon chloride cluster was isolated [64]. Owing to the complicated nature of the iron complexes of PDK⁴⁻, no further studies were pursued using this ligand.

The more pre-organized dicarboxylate ligands XDK²⁻ and Ph₄DBA²⁻ impart enhanced stability to their respective diiron complexes and allow detection of O₂ adducts at low temperature. A common problem with the dicarboxylate ligands, however, is that they do not prevent aggregation of the metal complexes into oligo- and polynuclear clusters [65], an undesired reaction that is detrimental to the synthesis of accurate models. Furthermore, the conformationally rigid ligand framework may be a liability in terms of accessing oxygenated diiron species that could further react with external substrates. During the reaction cycle of many non-heme diiron enzymes, "carboxylate shifts," or changes in the binding mode of carboxylate units to the diiron centers [66], are required for catalysis [67, 68]. Thus, devising a motif that

incorporates such “flexible” carboxylate groups into a ligand framework is an important synthetic goal.

2.3. Terphenylcarboxylate Ligands

To reduce the geometric constraints of the ligand platform, bulky terphenylcarboxylates were employed. Unlike simple benzoates that form polynuclear clusters with iron [69-71], the sterically hindered 2,6-bis(*p*-tolyl)benzoate ($\text{Ar}^{\text{Tol}}\text{CO}_2^-$, Table 1) and 2,6-bis(*p*-fluorophenyl)benzoate ($\text{Ar}^{4\text{-FPh}}\text{CO}_2^-$) ligands promote the self-assembly of discrete diiron compounds in the presence of iron salts and an appropriate base [72, 73]. The first iron complex synthesized in this series is $[\text{Fe}^{\text{II}}_2(\mu\text{-Ar}^{\text{Tol}}\text{CO}_2)_2(\text{Ar}^{\text{Tol}}\text{CO}_2)_2(\text{THF})_2]$ (**13**, THF = tetrahydrofuran), which adopts a “windmill” structure with two *syn,syn*-bridging carboxylates and two bidentate terminal carboxylates in the solid-state. The coordinated THF molecules in **13** can be readily substituted with *N*-donors to afford the corresponding $[\text{Fe}^{\text{II}}_2(\text{Ar}^{\text{Tol}}\text{CO}_2)_4(\text{N-donor})_2]$ complex. Use of 4-*tert*-butylpyridine (4-^tBuPy) as the ancillary base provided a quadruply bridged $[\text{Fe}^{\text{II}}_2(\text{Ar}^{\text{Tol}}\text{CO}_2)_4(4\text{-}^t\text{Bupy})_2]$ (**14A**, Table 1) “paddlewheel” compound. Interconversion between windmill (Scheme 2, **14C**) and paddlewheel (Scheme 2, **14A**) structures occurs in solution [66], as demonstrated by variable temperature NMR spectroscopic studies [73]. Oxygenation of **14A** at -78°C resulted in irreversible formation of a deep green intermediate that decayed to a $[\text{Fe}^{\text{III}}_2(\mu\text{-OH})_2(\mu\text{-Ar}^{\text{Tol}}\text{CO}_2)_2(\text{Ar}^{\text{Tol}}\text{CO}_2)_2(4\text{-}^t\text{Bupy})_2]$ (**17**) product [74, 75]. The di(μ -hydroxo)diiron(III) unit of **17** closely resembles that of the oxidized core of sMMOH [76]. Characterization of the green intermediate revealed two mixed-valent complexes, a diiron(II,III) (**15**) and a diiron(III,IV) (**16**) species, that are present in equal amounts. EPR and magnetic Mössbauer measurements indicated that **15** and **16** have spin states of 9/2 and 1/2, respectively. The assignment of **15** as a diiron(II,III) compound was confirmed by comparing its spectroscopic

properties to those of a crystallographically characterized $[\text{Fe}^{\text{II}}\text{Fe}^{\text{III}}(\text{Ar}^{\text{Tol}}\text{CO}_2)_4(4\text{-}^t\text{Bupy})_2]^+$ complex [77, 78]. As shown in the mechanism proposed in Scheme 2, reaction of **14A** with dioxygen proceeds through a carboxylate shift, in which either one or two of the bridging $\text{Ar}^{\text{Tol}}\text{CO}_2^-$ groups rearrange to adopt terminal positions, providing an open site for O_2 . Binding of dioxygen to **14B** or **14C** affords a (μ -peroxo)diiron(III) or a di(μ -oxo)diiron(IV) intermediate that further reacts with **14A**, giving an equal mixture of **15** and **16**. This reaction is noteworthy because it provides the first example for a synthetic model compound in which treatment of a diiron(II) precursor with O_2 resulted in formation of an iron(IV) species, a process that parallels the chemistry of several carboxylate-bridged diiron enzymes [17]. Oxygenation of diiron complexes derived from other terphenylcarboxylate ligand variants, such as 2,6-bis(mesityl)benzoate or 2,6-bis(dimethylbenzyl)-4-*tert*-butylbenzoate, have yielded (peroxo)diiron(III) species with distinct spectroscopic signatures. A detailed comparison of these latter systems with those studied in our laboratory is available [79].

Although the steric hindrance provided by the terphenylcarboxylates could suppress undesired reactions involving bond-making processes, it could not eliminate deleterious intermolecular electron transfer (ET) reactions [74, 75]. To prevent the paddlewheel diiron(II) complex from quenching the oxygenated intermediates, bidentate ancillary ligands were used to favor the assembly of windmill rather than paddlewheel species. The doubly-bridged $[\text{Fe}^{\text{II}}_2(\mu\text{-Ar}^{\text{Tol}}\text{CO}_2)_2(\text{Ar}^{\text{Tol}}\text{CO}_2)_2(N,N\text{-Bn}_2\text{en})_2]$ (**18**) complex, where $N,N\text{-Bn}_2\text{en} = N,N$ -dibenzylethylenediamine, was prepared to test this strategy [80, 81]. Compound **18** reacted with dioxygen, but instead of producing a green intermediate, *N*-dealkylation occurred affording $[\text{Fe}^{\text{III}}_2(\mu\text{-OH})_2(\mu\text{-Ar}^{\text{Tol}}\text{CO}_2)(\text{Ar}^{\text{Tol}}\text{CO}_2)_3(N\text{-Bnen})(N,N\text{-Bn}_2\text{en})]$ (**19**) (where $N\text{-Bnen} = N$ -benzylethylenediamine) and benzaldehyde. Isotopic labeling with $^{18}\text{O}_2$ demonstrated that the

oxygen atom in benzaldehyde was derived from O₂. When a non-coordinating *N,N*-Bn₂en analogue, such as *N,N*-dibenzylpropylamine, was treated with O₂ in the presence of either mononuclear or dinuclear iron(II) complexes, the yield of benzaldehyde was significantly reduced. Detailed mechanistic studies suggested that oxidative *N*-dealkylation of **18** involves single electron transfer, proton abstraction, and rearrangement [82, 83]. This fortuitous discovery that high-valent diiron terphenylcarboxylate complexes could be intercepted by *tethered substrates* inspired subsequent studies of the reactivity of oxygenated intermediates toward organic moieties held in close proximity to the diiron center. Attachment of benzyl [84, 85], ethyl [85], ethynyl [86], phenoxy [87], phosphido [84, 88], or sulfido [88, 89] units to an amine or pyridine ligand afforded a series of tethered substrates that could be easily incorporated into **13**, affording the corresponding diiron(II) compounds. After exposing the substrate/diiron(II) complex to O₂, the reaction products were analyzed by gas chromatography-mass spectrometry (GC-MS). Chart 1 depicts substrates that were successfully oxidized by this method. When 2-pyridyldiphenylphosphine (2-Ph₂Ppy) was employed in excess, catalytic oxidation to 2-pyridyldiphenylphosphine oxide (2-Ph₂P(O)py) was observed [84, 88]. Because external non-coordinating substrates cannot be oxidized by [Fe₂(Ar^{Tol}CO₂)₄(THF)₂]/O₂, these results suggest that intramolecular reactions are preferred over intermolecular ones in the terphenylcarboxylate diiron complexes. This behavior is most likely of the consequence of the formation of an active diiron oxidant that can react with solvent or adventitious reductants before being intercepted by the desired external substrates.

One strategy to prevent premature deactivation of an oxygenated diiron intermediate was to attach dendritic groups to the terphenylcarboxylate ligand to shield the diiron core from participating in intermolecular ET reactions [90]. The complex [Fe^{II}₂([G-3]CO₂)₄(4-CNpy)₂]

(**20**) (where [G-3]CO₂⁻ = third-generation dendrimer-appended terphenylcarboxylate and 4-CNpy = 4-cyanopyridine) was synthesized in a manner analogous to that for the simpler diiron(II) compounds. Treatment of **20** with dioxygen resulted in formation of a diiron(II,III) intermediate that was postulated to have a superoxo ligand. This colored intermediate is capable of oxidizing dihydroanthracene, albeit in only modest yields of up to ~40%.

The influence of water on the structure and reactivity of the diiron(II) terphenylcarboxylate compounds was also examined. Treatment of **14A** with excess water afforded a diaqua-bridged diiron(II) species, [Fe^{II}₂(μ-H₂O)₂(μ-Ar^{Tol}CO₂)₂(Ar^{Tol}CO₂)₂(4-*t*Bupy)₂] (**21**), in which the terminal carboxylates exhibit strong hydrogen-bonding interactions with the bridging waters [91]. In addition to having a diaqua bridge, a third H₂O molecule occupies a terminal position in [Fe^{II}₂(μ-H₂O)₂(μ-Ar^{4-FPh}CO₂)(Ar^{4-FPh}CO₂)₃(THF)₂(H₂O)] (**22**) [92]. When a large excess of water was added to **22**, complete dissolution occurred, giving the fully aquated [Fe^{II}(H₂O)₆]²⁺ cation. These observations suggest that the accessibility of water within diiron enzyme active sites may be a control element for achieving different functions using a common structural motif. The presence of excess amounts of water may be destructive to the integrity of the carboxylate-bridged diiron core, however. Stopped-flow kinetic studies using [Fe^{II}₂(μ-Ar^{Tol}CO₂)₄(4-CNpy)₂] (**23**) showed that it reacts with H₂O ~1000 times faster than with O₂ and that aquated **23** reacts with O₂ ~10 times faster than anhydrous **23** [93, 94]. Coordination of water to **23** most likely induces rearrangement from a paddlewheel to a windmill geometry, facilitating more rapid binding of dioxygen to the diiron center.

The iron chemistry of a variety of other monocarboxylate ligands was evaluated. When the steric bulk of the terphenylcarboxylate was increased using 2,6-bis(*p*-(*tert*-butyl)phenyl)-benzoate (Ar^{tBu}CO₂⁻), reaction with iron(II) salts afforded a tetrairon cluster [95]. When the

steric demand of the carboxylate was reduced using 2-biphenylcarboxylate, an assortment of di-, tri-, and tetranuclear species was obtained [96]. Replacing the terphenylcarboxylate with 9-triptycenecarboxylate resulted in diiron paddlewheel complexes that could not convert to the more reactive windmill structure [97].

Terphenylcarboxylate ligands are a simple alternative to the conformationally restricting dicarboxylate compounds. Diiron complexes derived from $\text{Ar}^{\text{Tol}}\text{CO}_2^-$ or $\text{Ar}^{4\text{-FPh}}\text{CO}_2^-$ can access high valent iron(IV) species from O_2 , which are capable of hydroxylating hydrocarbons, a first for synthetic modeling studies. Although the 2,6-aryl substituents of $\text{Ar}^{\text{Tol}}\text{CO}_2^-$ and $\text{Ar}^{4\text{-FPh}}\text{CO}_2^-$ are effective in shielding against metal cluster assembly, they also contribute to excessive steric crowding at the diiron core, which prevents facile entry of external substrates.

2.4. Dinucleating Polynitrogen Ligands

Polydentate nitrogen donors are commonly utilized as ligands in synthetic modeling studies [31, 98]. Although these compounds provide a nitrogen-, rather than a carboxylate-rich coordination environment they are well suited for stabilizing kinetically labile first row transition metal ions. Efforts to mimic the *syn, syn* coordination of the bridging carboxylate in the active site of diiron enzymes led to use of a naphthyridine framework as a “masked carboxylate” [99]. Several 1,8-substituted naphthyridine compounds were prepared and successfully employed to assemble dicopper(II), dizinc(II), dinickel(II), and diiron(II) complexes [100]. The most notable of these are $[\text{Fe}^{\text{II}}_2(\mu\text{-OH})(\text{BPEAN})(\text{SO}_3\text{CF}_3)]^{2+}$ (**24**, where BPEAN = 2,7-bis(bis(2-(2-(5-methylpyridyl)ethyl)aminomethyl)-1,8-naphthyridine, Table 1) and $[\text{Fe}^{\text{II}}_2(\mu\text{-OH})(\text{BEPEAN})(\text{SO}_3\text{CF}_3)]^{2+}$ (**25**, where BEPEAN = 2,7-bis(bis(2-(2-(5-ethylpyridyl)ethyl)aminomethyl)-1,8-naphthyridine) [101]. Exposing either **24** or **25** to O_2 at room temperature resulted in rapid decomposition without any detectable intermediates. When the

more sterically hindered **25** was treated with excess hydrogen peroxide at -30 °C a red-brown species (**26**) appeared, which decayed upon warming to room temperature. Spectroscopic characterization of **26** suggested that it is a (hydroperoxo)diiron(III) species. The decay of **26** is accompanied by O₂ evolution and formation of a diiron(II) unit, the identity of which is different from that of **25**. Although the mechanism of this reaction is uncertain, the release of O₂ from **26** may mimic a process similar to that in hemerythrin.

The stability of the diiron(II) naphthyridine compounds afforded an opportunity to investigate how the redox properties of the model complexes vary depending on their composition and structure. Because activation of O₂ in the diiron enzymes invariably results in oxidation of the metal center, knowledge of the redox potential of the diiron(II) models may help to explain their dioxygen reactivity. The cyclic voltammogram of [Fe^{II}₂(BPMAN)(μ-PhCyCO₂)₂]²⁺ (**27**, where BPMAN = 2,7-bis(bis(2-pyridylmethyl)aminomethyl)-1,8-naphthyridine) displayed two reversible redox waves at +296 and +681 mV (vs. ferrocene/ferrocenium) attributed to two one-electron oxidation processes, of diiron(II,II) to diiron(II,III) and diiron(II,III) to diiron(III,III), respectively [102]. The presence of two reversible metal-centered redox couples was unprecedented for diiron(II) compounds not having single atom bridge. Comparing the first oxidation potential of **27** to that of [Fe^{II}₂(Ar^{Tol}CO₂)₄(4-^tBupy)₂] (**14A**) (E_{1/2} = -216 mV) revealed that addition of each anionic carboxylate group *lowers* the redox potential of the diiron center by ~ 250 mV. These results also suggested that diiron(II) sites bridged only by Asp and Glu residues in biology could supply up to two electrons without significant change in geometry.

Another polynitrogen donor compound, 1,4-bis(2,2'-dipyridylmethyl)phthalazine (bdptz, Table 1), was explored as a potential dinucleating platform [103]. Reaction of bdptz with iron(II)

triflate and $\text{Ar}^{\text{Tol}}\text{CO}_2^-$ afforded a stable diiron(II) complex, $[\text{Fe}^{\text{II}}_2(\mu\text{-OH})(\mu\text{-Ar}^{\text{Tol}}\text{CO}_2)(\text{bdptz})(\text{CH}_3\text{CN})(\text{SO}_3\text{CF}_3)](\text{SO}_3\text{CF}_3)$ (**28**, Table 1). Treatment of **28** with dioxygen instantaneously led to formation of a (μ -oxo)diiron(III) product, $[\text{Fe}^{\text{III}}_2(\mu\text{-O})(\mu\text{-Ar}^{\text{Tol}}\text{CO}_2)(\text{bdptz})(\text{acetone})(\text{SO}_3\text{CF}_3)](\text{SO}_3\text{CF}_3)_2$ (**29**) with no detectable intermediates. A bulkier derivative of bdptz was prepared to block the possible formation of tetranuclear species, but no remarkable oxygenation chemistry was observed with the diiron complex of this compound [104].

Although the naphthyridine and phthalazine bridged diiron model complexes are structurally robust, they do not exhibit the same O_2 reactivity observed in the diiron proteins. Perhaps polydentate ligands with internal bridging units are too rigid to accommodate binding of O_2 to the diiron center.

2.5. Syn *N*-Donor Ligands

An important structural feature that has been difficult to reproduce in carboxylate-bridged diiron model complexes is the syn coordination of nitrogen donors relative to the iron-iron vector (Scheme 1) [31]. Despite the different arrangement of carboxylate ligands within the active sites of the BMMs, RNR, and related enzymes, ligation of the two histidine residues always occurs with syn stereochemistry [17]. To enforce the syn arrangement of nitrogen donors within a single ligand framework, two quinoline ester moieties were covalently attached using a diethynylbenzene linker, giving 1,2-bis(3-ethynyl-8-carboxylatequinoline)-4,5-diethynylbenzene ethyl ester ($\text{Et}_2\text{BCQEB}^{\text{Et}}$, Table 1) [105]. Metallation of $\text{Et}_2\text{BCQEB}^{\text{Et}}$ using iron(II) triflate and $\text{Ar}^{\text{Tol}}\text{CO}_2^-$ afforded the compound $[\text{Fe}^{\text{II}}_2(\text{Et}_2\text{BCQEB}^{\text{Et}})(\mu\text{-Ar}^{\text{Tol}}\text{CO}_2)_3]^+$ (**30**, Table 1). X-ray structural analysis of **30** revealed a diiron complex with three bridging carboxylates and syn binding of the quinoline moieties. Although **30** is a close structural mimic of $\text{sMMOH}_{\text{red}}$ (Scheme 1, bottom) [76], exposing the compound to dioxygen resulted in iron products that

could not be identified. Other neutral derivatives of $\text{Et}_2\text{BCQEB}^{\text{Et}}$ were prepared and examined as syn *N*-donor ligands [106]. The compound bis(picolinic methyl ester)diethynyltriptycene (PIC_2DET) containing pyridine methyl ester groups afforded a heterometallic $[\text{Fe}^{\text{II}}\text{Na}(\text{PIC}_2\text{DET})(\mu\text{-TrpCO}_2)_3]$ (**31**) complex that could exchange sodium for iron; the resulting diiron(II) compound could not be structurally characterized, however [107]. Two syn *N*-donor ligands can also bridge two iron(II) centers, giving $[\text{Fe}^{\text{II}}_2(\text{syn } N\text{-donor})_2]$ species [108]. Several examples are shown in Chart 2 [S. Friedle, L.H. Do, S.J. Lippard, Unpublished work]. Such undesired $[\text{Fe}^{\text{II}}_2(\text{syn } N\text{-donor})_2]$ species were avoided by the use of ligands bearing polydentate nitrogen-rich metal binding groups [109]. Only diiron(III) complexes, however, could be prepared from these ligands.

To obtain a kinetically more stabilizing platform, 2-phenoxyypyridine groups were attached to a 1,2-diethynylbenzene backbone [110]. Reaction of bis(phenyl(*p*-cresol)pyridyl)-diethynylbenzene ($[\text{L}^{\text{Me,Ph}}]^{2-}$) with iron(II) in THF led to spontaneous formation of $[\text{Fe}^{\text{II}}_2(\text{L}^{\text{Me,Ph}})_2(\text{THF})_3]$ (**32D**, Chart 2). Once again, rotation about the C–C bond of the ethynyl arms allowed association of two syn *N*-donor ligands. Unlike complex **30**, however, reaction of **32D** with dioxygen resulted in the quantitative formation of a (μ -oxo)diiron(III) $[\text{Fe}^{\text{III}}_2(\mu\text{-O})(\text{L}^{\text{Me,Ph}})_2]$ (**33**) product. No intermediates were detected during the oxygenation reaction.

Several other ligand designs based on the syn *N*-donor concept were also explored. An attempt was made to incorporate both a bridging carboxylate and adjacent amine moieties into a dinucleating platform using 1,8-bis(dimethylaminomethylethynyl)-3,6-di(*tert*-butyl)fluorene-9-yl-acetate (DAFA^{2-} , Table 1) [111]. Efforts to metallate DAFA^{2-} with iron(II) were unsuccessful, possibly due to a lack of pre-organization among the amine and carboxylate donor groups of the ligand. A two-component system was also proposed as a method to assemble

diiron(II) model complexes. In addition to a syn *N*-donor, a “C-clamp” ligand with two *endo*-oriented dicarboxylate groups may enforce a doubly-bridging motif and form a hydrophobic pocket around the diiron center [112]. Complexation reactions with a C-clamp and syn *N*-donor ligands have not yet afforded the desired $[\text{Fe}^{\text{II}}_2(\text{syn } N\text{-donor})(\text{C-clamp})]$ unit, however.

Linking two *N*-heterocycles with a 1,2-diethynylarene spacer effectively enforces the syn coordination of nitrogen donors in a diiron complex. Because the compounds do not have an internal bridging group to link the two metal ions like other dinucleating ligands, their terminal metal-binding units must be sufficiently stabilizing to prevent dissociation of the dinuclear core. Additional ligand modifications are needed to eliminate the possibility of forming $[\text{Fe}^{\text{II}}_2(\text{syn } N\text{-donor})_2]$ species.

2.6. Macrocyclic Ligands

Macrocyclic ligands are excellent hosts for transition metal ions, as evident from numerous examples in biology [3, 4] as well as synthetic coordination chemistry [113, 114]. Initial efforts to prepare a dinucleating macrocycle led to synthesis of a bis(terphenylcarboxylate) compound linked by 1,3-bis(aminomethyl)-4,6-diisopropylbenzene ($\text{MAr}^{\text{Tol}}\text{CO}_2^{2-}$, Table 1) [115]. The *endo*-carboxylate groups in $\text{MAr}^{\text{Tol}}\text{CO}_2^{2-}$ were designed to bridge two iron atoms to form a pre-organized platform for binding of additional external ligands. The failure to complex $\text{MAr}^{\text{Tol}}\text{CO}_2^{2-}$ with iron, however, was attributed to either the flexibility of the ligand architecture or improper spacing provided by the phenylene linker.

An improved macrocyclic design was obtained with the compound PIM^{2-} (Table 1), which contains two phenoxyimine metal binding units linked by diphenylsulfone and dibenzylether moieties [116]. Reaction of H_2PIM , the protonated form of PIM^{2-} , with $[\text{Fe}^{\text{II}}_2(2,4,6\text{-trimethylphenyl})_4]$ and sterically hindered carboxylic acid afforded di(μ -

carboxylato)diiron(II) complexes in good yield. Use of terphenylcarboxylic acid and triphenylacetic acid gave $[\text{Fe}^{\text{II}}_2(\mu\text{-Ar}^{\text{Tol}}\text{CO}_2)_2(\text{PIM})]$ (**34**, Table 1) and $[\text{Fe}^{\text{II}}_2(\mu\text{-Ph}_3\text{CCO}_2)_2(\text{PIM})]$ (**35**), respectively. X-ray structural analysis revealed that both compounds accurately mimic the active site structure of sMMOH_{red} (Scheme 1, bottom) [76], including the asymmetric $\mu\text{-}\eta^1, \eta^1$ and $\mu\text{-}\eta^1, \eta^2$ binding mode of carboxylates as well as the syn stereochemistry of nitrogen donors. When **34** was exposed to dioxygen, a mixture of ($\mu\text{-oxo}$)diiron(III) $[\text{Fe}^{\text{III}}_2(\mu\text{-O})(\text{Ar}^{\text{Tol}}\text{CO}_2)_2(\text{PIM})]$ (**36**) and di($\mu\text{-hydroxo}$)diiron(III) $[\text{Fe}^{\text{III}}_2(\mu\text{-OH})_2(\text{Ar}^{\text{Tol}}\text{CO}_2)_2(\text{PIM})]$ (**37**) species was isolated. Further treatment of **36** and **37** with excess water resulted in dimerization of the complexes to form tetranuclear $[\text{Fe}^{\text{III}}_4(\mu\text{-OH})_6(\text{PIM})_2(\text{Ar}^{\text{Tol}}\text{CO}_2)_2]$ (**38**) species. To eliminate this decomposition pathway, the PIM^{2-} ligand could be modified with sterically more hindering groups at the *para* position of the phenolate (Scheme 3). Having a more bulky platform would also allow smaller carboxylate ligands to be employed, which may facilitate dioxygen binding or substrate access to the diiron center. Unlike other platforms that have been investigated to date, the planar nature of the macrocycle allows for steric tuning of the diiron complex without obstructing access to the dimetallic center.

3. Concluding Remarks

The early years of synthetic modeling of carboxylate-bridged diiron protein active sites in our laboratory were characterized by use of simple chelating ligands to prepare structural mimics. Efforts to replicate the functional aspects of these proteins, however, required more elaborately designed ligands. The search for an ideal synthetic platform is complicated by a number of factors, such as the need for ligands that can complex two iron atoms to afford the desired coordination geometry, tune the ligand steric properties to prevent unproductive decomposition of reactive oxygenated species, and develop short and convenient routes to target compounds in significant quantities. Although there is no substitute for direct studies of biomolecules, the work described in this summary illustrates that investigations using synthetic mimics can provide insight into metallobiochemistry in ways that could not be achieved through other means.

Synthetic diiron modeling still offers many unexplored frontiers. One area of interest is understanding the chemical nature as well as the requirements for generating potent oxidizing diiron units. One strategy to access such chemically reactive species is to prepare diiron complexes that have optimally positioned functional groups to stabilize key transition states along the O₂ reaction pathway. Identifying which transition state structures to target can be aided by the use of quantum mechanical calculations [117, 118]. This concept has been successfully demonstrated in de novo protein design [119-121], but has not yet been seriously applied to construct small-molecule protein models. Use of outer sphere coordination to influence the reactivity of metalcenters is well documented in biology [122]. For example, recent studies of toluene/*o*-xylene monooxygenase hydroxylase (ToMOH), a member of the BMM family, suggest that a threonine residue in the second coordination sphere of the protein active site

facilitates formation of a (μ - η^1, η^1 -hydroperoxo)diiron(III) species through proton transfer and hydrogen bonding to the coordinated dioxygen ligand [123, 124]. This interaction, although subtle, may help explain why the (peroxo)diiron(III) intermediate of ToMOH has characteristics that are distinct from those of sMMOH. Another avenue of research that would help advance diiron modeling chemistry is to establish a clear structure-function relationship between the model compounds and their oxygenation behavior [125]. For example, although it has been shown that exposing dioxygen to a synthetic diiron(II) complex can lead to formation of a (peroxo)diiron(III) species, this reactivity is not general to all diiron(II) model compounds. In many cases, it is unclear whether oxygenated diiron units are not observed because they are rapidly quenched by external reactants, do not form under the experimental conditions employed, or the starting complexes are too sterically hindered to bind O₂. To evaluate the various factors that contribute to the dioxygen reactivity in a synthetic model, it is necessary to make systematic structural and electronic modifications to the complex. Unfortunately, most model systems are not amenable to such investigations because the structural integrity of the complexes may be compromised upon introducing such changes. Because PIM²⁻ is a remarkably robust dinucleating platform and has many potential sites for derivatization, it is an excellent framework for such studies.

Although this review has focused exclusively on diiron modeling chemistry in our laboratory, many other research groups have made significant contributions to the development of carboxylate-bridged diiron protein model complexes and the investigation of their chemical and physical characteristics. A large number of synthetic platforms have been devised for the assembly of carboxylate-bridged diiron model complexes, ranging from simple carboxylate/pyridine [126] donors to tailored-made dinucleating ligands [31, 127] and synthetic

peptides [128, 129]. Although many of the diiron model compounds reported are structurally robust [31, 127], they do not capture the unique coordination sphere of the bioinorganic unit of interest. Perhaps as a consequence of the incomplete match, the synthetic complexes do not typically exhibit the same reactivity profile as that of the diiron proteins [35, 130]. It is unlikely that every element of a protein active site, including the second coordination sphere, can be reproduced in a single model system. But given the extent of the synthetic methodologies available today, it should be possible to overcome many of the obstacles that have impeded the development of more sophisticated diiron protein mimics [32].

Extensive reactivity studies utilizing molecular oxygen, hydrogen peroxide, alkyl peroxides, and oxygen atom transfer reagents with diiron model compounds have led to a much improved understanding of the oxidation chemistry that takes place in the active sites of carboxylate-bridged diiron proteins [32, 36]. For example, characterization of diiron(III,IV) and diiron(IV,IV) species in synthetic models [131-134] has shed some light on similar high-valent states that are accessible within the diiron protein cores. These achievements help us to formulate possible reaction schemes that reconcile the biochemical data [17, 18] with the proposed biological mechanisms suggested by theory [67, 68, 135, 136]. Beyond the O₂ activation step, some synthetic systems are even able to perform catalytic hydrocarbon oxidation [34, 137, 138]. Although these reactions are typically not as efficient as those catalyzed by the bacterial monooxygenases, they represent a good start. The current challenge in diiron model chemistry is to achieve regio- and stereospecific oxidation of external substrates by non-“free radical” reaction pathways. Use of the earth-abundant molecule dioxygen, rather than other more reactive but environmentally less friendly chemical oxidants, to facilitate this chemistry is the ultimate goal. The tasks set forth for future researchers in biomimetic modeling are

numerous and complex, but the advances that have been made over the past thirty years promise a future that is full of many exciting discoveries.

4. Table of Abbreviations

2-Ph ₂ P(O)py	2-pyridyldiphenylphosphine oxide
2-Ph ₂ Py	2-pyridyldiphenylphosphine
3-Fpy	3-fluoropyridine
4- ^t Bupy	4- <i>tert</i> -butylpyridine
4-CNpy	4-cyanopyridine
[G3]CO ₂ ⁻	third generation dendrimer appended terphenylcarboxylate
[L ^{Me,Ph}] ²⁻	anion of bis(phenyl(<i>p</i> -cresol)pyridyl)diethynylbenzene
Ar ^{4-FPh} CO ₂ ⁻	2,6-bis(<i>p</i> -fluorophenyl)benzoate
Ar ^{tBu} CO ₂ ⁻	2,6-bis(<i>p</i> -(<i>tert</i> -butyl)phenyl)benzoate
Ar ^{Tol} CO ₂ ⁻	2,6-bis(<i>p</i> -tolyl)benzoate
bdptz	1,4-bis(2,2'-dipyridylmethyl)phthalazine
BEPEAN	2,7-bis(bis(2-(2-(5-ethyl)pyridyl)ethyl)aminomethyl)-1,8-naphthyridine
BIPhMe	bis(1-methylimidazol-2-yl)phenylmethoxymethane
BMMs	bacterial multi-component monooxygenases
BPEAN	2,7-bis(bis(2-(2-(5-methyl)pyridyl)ethyl)aminomethyl)-1,8-naphthyridine
BPMAN	2,7-bis(bis(2-pyridylmethyl)aminomethyl)-1,8-naphthyridine
bpy	2,2'-bipyridine
BXDK ²⁻	benzyl substituted variant of XDK ²⁻
CV	cyclic voltammetry
deoxyHr	reduced form of hemerythrin, with no dioxygen bound
DAFA ²⁻	1,8-bis(dimethylaminomethylethynyl)-3,6-di(<i>tert</i> -butyl)fluorine-9-yl-acetate
DFT	density functional theory
ET	electron transfer

Et ₂ BCQEB ^{Et}	1,2-bis(3-ethynyl-8-carboxylatequinoline)-4,5-diethynylbenzene methyl ester
EXAFS	extended X-ray absorption fine structure
Hr	hemerythrin
Im ₂ DET	bis(<i>N</i> -methylimidazole)diethynyltriptycene
<i>i</i> PrCO ₂ ⁻	isobutyrate
Lut	2,6-lutidine
MAr ^{Tol} CO ₂ ²⁻	1,3-bis(aminomethyl)-4,6-diisopropylbenzene linked bis(terphenylcarboxylate)
Mes	2,4,6-trimethylphenyl
MPDP ²⁻	<i>m</i> -phenylenedipropionate
NADH	the reduced form of nicotinamide adenine dinucleotide
<i>N</i> -MeIm	<i>N</i> -methylimidazole
<i>N,N</i> -Bn ₂ en	<i>N,N</i> -dibenzylethylenediamine
<i>N-t</i> BuIm	<i>N-tert</i> -butylimidazole
oxyHr	dioxygen-bound form of hemerythrin
PDK ⁴⁻	anion of α,α -5,15-bis(α - <i>N</i> -(Kemp's triacid imido)- <i>o</i> -tolyl)-2,8,12,18-tetraethyl-3,7,13,17-tetramethylporphyrin
PIC ₂ DET	bis(picolinic methyl ester)diethynyltriptycene
PIM ²⁻	dibenzylether linked bis(3-(methylphenoxyimine)phenyl)sulfone
Ph ₄ DBA ²⁻	dibenzofuran-4,6-bis(diphenylacetate)
PhCO ₂ ⁻	benzoate
PhCyCO ₂ ⁻	1-phenylcyclohexylcarboxylate
PXDK ²⁻	propyl substituted variant of XDK ²⁻
py	pyridine
R2	ribonucleotide reductase subunit containing the diiron active site
RNR	ribonucleotide reductase
sMMOH	soluble methane monooxygenase hydroxylase

$t\text{-BuCH}_2\text{CO}_2^-$	1- <i>tert</i> -butylacetate
$t\text{-BuCO}_2^-$	pivalate
THF	tetrahydrofuran
TMEDA	<i>N,N,N',N'</i> -tetramethylethylenediamine
ToMOH	toluene/ <i>o</i> -xylene monooxygenase hydroxylase
TP ⁻	hydrotris(pyrazolyl)borate
XDK ²⁻	anion of <i>m</i> -xylenediamine bis(Kemp's triacid)imide

5. Acknowledgements

We wish to acknowledge all the graduate students and postdoctoral associates in our laboratory as well as many collaborators who have contributed to the synthetic diiron modeling project over the years. We gratefully acknowledge the National Institute of General Medical Sciences for long-term support of this research.

6. References

- [1] R.J.P. Williams, *Coord. Chem. Rev.* 100 (1990) 573-610.
- [2] R.H. Holm, P. Kennepohl, E.I. Solomon, *Chem. Rev.* 96 (1996) 2239-2314.
- [3] I. Bertini, H.B. Gray, S.J. Lippard, J.S. Valentine, *Bioinorganic Chemistry*, Mill Valley: University Science Books, 1994.
- [4] S.J. Lippard, J.M. Berg, *Principles of Bioinorganic Chemistry*, Mill Valley: University Science Books; 1994.
- [5] L. Que, Jr., *Physical Methods in Bioinorganic Chemistry: Spectroscopy and Magnetism*, Sausalito, CA: University Science Books, 2000.
- [6] R. Vilar, *Annu. Rep. Sect. A* 105 (2009) 477-504.

- [7] B. Kirchner, F. Wennmohs, S. Ye, F. Neese, *Curr. Opin. Chem. Biol.* 11 (2007) 134-141.
- [8] J. Chatt, J.R. Dilworth, R.L. Richards, *Chem. Rev.* 78 (1978) 589-625.
- [9] J.B. Howard, D.C. Rees, *Chem. Rev.* 96 (1996) 2965-2982.
- [10] I. Dance, *Dalton Trans.* 39 (2010) 2972-2983.
- [11] R.R. Schrock, *Acc. Chem. Res.* 38 (2005) 955-962.
- [12] A. Williamson, B. Conlan, W. Hillier, T. Wydrzynski, *Photosyn. Res.* 107 (2011) 71-86.
- [13] J.C. Gordon, G.J. Kubas, *Organometallics* 29 (2010) 4682-4701.
- [14] N.S. Lewis, D.G. Nocera, *Proc. Natl. Acad. Sci. U.S.A.* 103 (2006) 15729-15735.
- [15] K.C. Nicolaou, D. Vourloumis, N. Winssinger, P.S. Baran, *Angew. Chem., Int. Ed.* 39 (2000) 44-122.
- [16] S.J. Lippard, *Nature* 416 (2002) 587.
- [17] A.L. Feig, S.J. Lippard, *Chem. Rev.* 94 (1994) 759-805.
- [18] B.J. Wallar, J.D. Lipscomb, *Chem. Rev.* 96 (1996) 2625-2658.
- [19] R.E. Stenkamp, *Chem. Rev.* 94 (1994) 715-726.
- [20] P. Nordlund, P. Reichard, *Annu. Rev. Biochem.* 75 (2006) 681-706.
- [21] J.G. Leahy, P.J. Batchelor, S.M. Morcomb, *FEMS Microbiol. Rev.* 27 (2003) 449-479.
- [22] K.E. Liu, A.M. Valentine, D. Wang, B.H. Huynh, D.E. Edmondson, A. Salifoglou, S.J. Lippard, *J. Am. Chem. Soc.* 117 (1995) 10174-10185.
- [23] P. Moënne-Loccoz, J. Baldwin, B.A. Ley, T.M. Loehr, J.M. Bollinger, Jr., *Biochemistry* 37 (1998) 14659-14663.
- [24] B.J. Brazeau, J.D. Lipscomb, *Biochemistry* 39 (2000) 13503-13515.
- [25] L.J. Murray, S.G. Naik, D.O. Ortillo, R. García-Serres, J.K. Lee, B.H. Huynh, S.J. Lippard, *J. Am. Chem. Soc.* 129 (2007) 14500-14510.

- [26] L. Shu, J.C. Nesheim, K. Kauffmann, E. Münck, J.D. Lipscomb, L. Que, Jr., *Science* 275 (1997) 515-518.
- [27] M. Merckx, D.A. Kopp, M.H. Sazinsky, J.L. Blazyk, J. Müller, S.J. Lippard, *Angew. Chem., Int. Ed.* 40 (2001) 2782-2807.
- [28] V.K. Korboukh, N. Li, E.W. Barr, J.M. Bollinger, Jr., C. Krebs, *J. Am. Chem. Soc.* 131 (2009) 13608-13609.
- [29] V.V. Vu, J.P. Emerson, M. Martinho, Y.S. Kim, E. Münck, M.H. Park, L. Que, Jr., *Proc. Natl. Acad. Sci. U.S.A.* 106 (2009) 14814-14819.
- [30] R.K. Behan, S.J. Lippard, *Biochemistry* 49 (2010) 9679-9681.
- [31] E.Y. Tshuva, S.J. Lippard, *Chem. Rev.* 104 (2004) 987-1012.
- [32] L. Que, Jr., W.B. Tolman, *Nature* 455 (2008) 333-340.
- [33] L. Que, Jr., *Dalton Trans.* (1997) 3933-3940.
- [34] M. Fontecave, S. Ménage, C. Duboc-Toia, *Coord. Chem. Rev.* 178-180 (1998) 1555-1572.
- [35] S. Friedle, E. Reisner, S.J. Lippard, *Chem. Soc. Rev.* 39 (2010) 2768-2779.
- [36] J. Du Bois, T.J. Mizoguchi, S.J. Lippard, *Coord. Chem. Rev.* 200-202 (2000) 443-485.
- [37] W.H. Armstrong, S.J. Lippard, *J. Am. Chem. Soc.* 105 (1983) 4837-4838.
- [38] W.H. Armstrong, A. Spool, G.C. Papaefthymiou, R.B. Frankel, S.J. Lippard, *J. Am. Chem. Soc.* 106 (1984) 3653-3667.
- [39] W.H. Armstrong, S.J. Lippard, *J. Am. Chem. Soc.* 106 (1984) 4632-4633.
- [40] A. Spool, I.D. Williams, S.J. Lippard, *Inorg. Chem.* 24 (1985) 2156-2162.
- [41] B. Hedman, M.S. Co, W.H. Armstrong, K.O. Hodgson, S.J. Lippard, *Inorg. Chem.* 25 (1986) 3708-3711.
- [42] W.B. Tolman, A. Bino, S.J. Lippard, *J. Am. Chem. Soc.* 111 (1989) 8522-8523.

- [43] W.B. Tolman, S. Liu, J.G. Bentsen, S.J. Lippard, *J. Am. Chem. Soc.* 113 (1991) 152-164.
- [44] R.H. Beer, W.B. Tolman, S.G. Bott, S.J. Lippard, *Inorg. Chem.* 28 (1989) 4557-4558.
- [45] R.H. Beer, W.B. Tolman, S.G. Bott, S.J. Lippard, *Inorg. Chem.* 30 (1991) 2082-2092.
- [46] J. Rebek, Jr., L. Marshall, R. Wolak, K. Parris, M. Killoran, B. Askew, D. Nemeth, N. Islam, *J. Am. Chem. Soc.* 107 (1985) 7476-7481.
- [47] L. Marshall, K. Parris, J. Rebek, Jr., S.V. Luis, M.I. Burguete, *J. Am. Chem. Soc.* 110 (1988) 5192-5193.
- [48] K.S. Hagen, R. Lachicotte, A. Kitaygorodskiy, A. Elbouadili, *Angew. Chem., Int. Ed.* 32 (1993) 1321-1324.
- [49] D.P. Goldberg, S.P. Watton, A. Masschelein, L. Wimmer, S.J. Lippard, *J. Am. Chem. Soc.* 115 (1993) 5346-5347.
- [50] D.P. Goldberg, D. Koulougliotis, G.W. Brudvig, S.J. Lippard, *J. Am. Chem. Soc.* 117 (1995) 3134-3144.
- [51] T. Tanase, S.P. Watton, S.J. Lippard, *J. Am. Chem. Soc.* 116 (1994) 9401-9402.
- [52] S.P. Watton, A. Masschelein, J. Rebek, Jr., S.J. Lippard, *J. Am. Chem. Soc.* 116 (1994) 5196-5205.
- [53] T.J. Mizoguchi, S.J. Lippard, *Inorg. Chem.* 36 (1997) 4526-4533.
- [54] S. Herold, L.E. Pence, S.J. Lippard, *J. Am. Chem. Soc.* 117 (1995) 6134-6135.
- [55] S. Herold, S.J. Lippard, *J. Am. Chem. Soc.* 119 (1997) 145-156.
- [56] D.D. LeCloux, A.M. Barrios, T.J. Mizoguchi, S.J. Lippard, *J. Am. Chem. Soc.* 120 (1998) 9001-9014.
- [57] D.D. LeCloux, A.M. Barrios, S.J. Lippard, *Bioorg. Med. Chem.* 7 (1999) 763-772.
- [58] L.G. Beauvais, S.J. Lippard, *J. Am. Chem. Soc.* 127 (2005) 7370-7378.

- [59] L.G. Beauvais, S.J. Lippard, *Biochem. Biophys. Res. Commun.* 338 (2005) 262-266.
- [60] T.J. Mizoguchi, S.J. Lippard, *J. Am. Chem. Soc.* 120 (1998) 11022-11023.
- [61] T.J. Mizoguchi, J. Kuzelka, B. Spingler, J.L. DuBois, R.M. Davydov, B. Hedman, K.O. Hodgson, S.J. Lippard, *Inorg. Chem.* 40 (2001) 4662-4673.
- [62] X.-X. Zhang, S.J. Lippard, *J. Org. Chem.* 65 (2000) 5298-5305.
- [63] X.-X. Zhang, P. Fuhrmann, S.J. Lippard, *J. Am. Chem. Soc.* 120 (1998) 10260-10261.
- [64] X.-X. Zhang, S.J. Lippard, *Inorg. Chem.* 39 (2000) 4388-4389.
- [65] S.P. Watton, P. Fuhrmann, L.E. Pence, A. Caneschi, A. Cornia, G.L. Abbati, S.J. Lippard, *Angew. Chem., Int. Ed.* 36 (1997) 2774-2776.
- [66] R.L. Rardin, W.B. Tolman, S.J. Lippard, *New J. Chem.* 15 (1991) 417-430.
- [67] B.D. Dunietz, M.D. Beachy, Y. Cao, D.A. Whittington, S.J. Lippard, R.A. Friesner, *J. Am. Chem. Soc.* 122 (2000) 2828-2839.
- [68] D. Rinaldo, D.M. Philipp, S.J. Lippard, R.A. Friesner, *J. Am. Chem. Soc.* 129 (2007) 3135-3147.
- [69] W. Micklitz, S.J. Lippard, *Inorg. Chem.* 27 (1988) 3067-3069.
- [70] W. Micklitz, V. McKee, R.L. Rardin, L.E. Pence, G.C. Papaefthymiou, S.G. Bott, S.J. Lippard, *J. Am. Chem. Soc.* 116 (1994) 8061-8069.
- [71] P. Ammala, J.D. Cashion, C.M. Kepert, B. Moubaraki, K.S. Murray, L. Spiccia, B.O. West, *Angew. Chem., Int. Ed.* 39 (2000) 1688-1690.
- [72] D. Lee, S.J. Lippard, *J. Am. Chem. Soc.* 120 (1998) 12153-12154.
- [73] D. Lee, S.J. Lippard, *Inorg. Chem.* 41 (2002) 2704-2719.
- [74] D. Lee, J. Du Bois, D. Petasis, M.P. Hendrich, C. Krebs, B.H. Huynh, S.J. Lippard, *J. Am. Chem. Soc.* 121 (1999) 9893-9894.

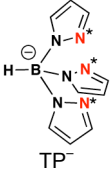
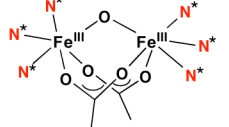

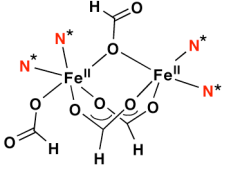

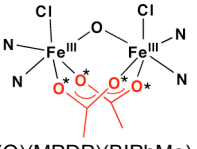
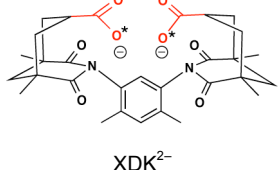
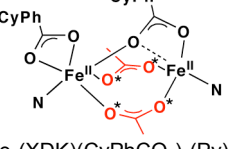
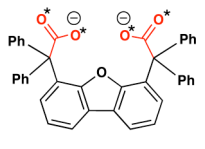
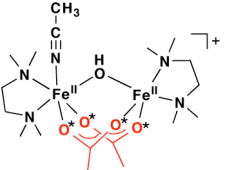
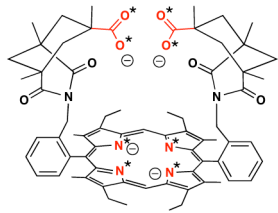
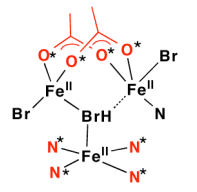
- [75] D. Lee, B. Pierce, C. Krebs, M.P. Hendrich, B.H. Huynh, S.J. Lippard, *J. Am. Chem. Soc.* 124 (2002) 3993-4007.
- [76] A.C. Rosenzweig, P. Nordlund, P.M. Takahara, C.A. Frederick, S.J. Lippard, *Chem. Biol.* 2 (1995) 409-418.
- [77] D. Lee, C. Krebs, B.H. Huynh, M.P. Hendrich, S.J. Lippard, *J. Am. Chem. Soc.* 122 (2000) 5000-5001.
- [78] D. Lee, J.L. DuBois, B. Pierce, B. Hedman, K.O. Hodgson, M.P. Hendrich, S.J. Lippard, *Inorg. Chem.* 41 (2002) 3172-3182.
- [79] W.B. Tolman, L. Que, Jr., *J. Chem. Soc., Dalton Trans.* (2002) 653-660.
- [80] D. Lee, S.J. Lippard, *J. Am. Chem. Soc.* 123 (2001) 4611-4612.
- [81] D. Lee, S.J. Lippard, *Inorg. Chem.* 41 (2002) 827-837.
- [82] S. Yoon, S.J. Lippard, *Inorg. Chem.* 42 (2003) 8606-8608.
- [83] S. Yoon, S.J. Lippard, *Inorg. Chem.* 45 (2006) 5438-5446.
- [84] E.C. Carson, S.J. Lippard, *J. Am. Chem. Soc.* 126 (2004) 3412-3413.
- [85] E.C. Carson, S.J. Lippard, *Inorg. Chem.* 45 (2006) 828-836.
- [86] E.C. Carson, S.J. Lippard, *J. Inorg. Biochem.* 100 (2006) 1109-1117.
- [87] S. Friedle, S.J. Lippard, *Eur. J. Inorg. Chem.* (2009) 5506-5515.
- [88] E.C. Carson, S.J. Lippard, *Inorg. Chem.* 45 (2006) 837-848.
- [89] E. Reisner, T.C. Abikoff, S.J. Lippard, *Inorg. Chem.* 46 (2007) 10229-10240.
- [90] M. Zhao, B. Helms, E. Slonkina, S. Friedle, D. Lee, J. DuBois, B. Hedman, K.O. Hodgson, J.M. Fréchet, S.J. Lippard, *J. Am. Chem. Soc.* 130 (2008) 4352-4363.
- [91] S. Yoon, A.E. Kelly, S.J. Lippard, *Polyhedron* 23 (2004) 2805-2812.
- [92] S. Yoon, S.J. Lippard, *J. Am. Chem. Soc.* 126 (2004) 16692-16693.

- [93] S. Yoon, S.J. Lippard, *J. Am. Chem. Soc.* 127 (2005) 8386-8397.
- [94] M. Zhao, D. Song, S.J. Lippard, *Inorg. Chem.* 45 (2006) 6323-6330.
- [95] D. Lee, L. Sorace, A. Caneschi, S.J. Lippard, *Inorg. Chem.* 40 (2001) 6774-6781.
- [96] E. Reisner, J. Telser, S.J. Lippard, *Inorg. Chem.* 46 (2007) 10754-10770.
- [97] S. Friedle, J.J. Kodanko, K.L. Fornace, S.J. Lippard, *J. Mol. Struct.* 890 (2008) 317-327.
- [98] E.A. Lewis, W.B. Tolman, *Chem. Rev.* 104 (2004) 1047-1076.
- [99] C. He, S.J. Lippard, *Tetrahedron* 56 (2000) 8245-8252.
- [100] C. He, S.J. Lippard, *J. Am. Chem. Soc.* 122 (2000) 184-185.
- [101] C. He, A.M. Barrios, D. Lee, J. Kuzelka, R.M. Davydov, S.J. Lippard, *J. Am. Chem. Soc.* 122 (2000) 12683-12690.
- [102] C. He, S.J. Lippard, *Inorg. Chem.* 40 (2001) 1414-1420.
- [103] A.M. Barrios, S.J. Lippard, *Inorg. Chem.* 40 (2001) 1060-1064.
- [104] J. Kuzelka, B. Spingler, S.J. Lippard, *Inorg. Chim. Acta* 337 (2002) 212-222.
- [105] J. Kuzelka, J.R. Farrell, S.J. Lippard, *Inorg. Chem.* 42 (2003) 8652-8662.
- [106] J.J. Kodanko, A.J. Morys, S.J. Lippard, *Org. Lett.* 7 (2005) 4585-4588.
- [107] J.J. Kodanko, D. Xu, D. Song, S.J. Lippard, *J. Am. Chem. Soc.* 127 (2005) 16004-16005.
- [108] J.J. Kodanko, S.J. Lippard, *Inorg. Chim. Acta* 361 (2008) 894-900.
- [109] S. Friedle, J.J. Kodanko, A.J. Morys, T. Hayashi, P. Moënne-Loccoz, S.J. Lippard, *J. Am. Chem. Soc.* 131 (2009) 14508-14520.
- [110] L.H. Do, S.J. Lippard, *Inorg. Chem.* 48 (2009) 10708-10719.
- [111] D. Burdinski, K. Cheng, S.J. Lippard, *Tetrahedron* 61 (2005) 1587-1594.
- [112] E. Reisner, S.J. Lippard, *Eur. J. Org. Chem.* (2008) 156-163.
- [113] S.J. Archibald, *Annu. Rep. Sect. A* 103 (2007) 264-286.

- [114] D.H. Busch, *Acc. Chem. Res.* 11 (1978) 392-400.
- [115] J.R. Farrell, D. Stiles, W. Bu, S.J. Lippard, *Tetrahedron* 59 (2003) 2463-2469.
- [116] L.H. Do, S.J. Lippard, *J. Am. Chem. Soc.* 133 (2011) 10568-10581.
- [117] D.J. Tantillo, C. Jiangang, K.N. Houk, *Curr. Opin. Chem. Biol.* 2 (1998) 743-750.
- [118] X. Zhang, J. DeChancie, H. Gunaydin, A.B. Chowdry, F.R. Clemente, A.J.T. Smith, T.M. Handel, K.N. Houk, *J. Org. Chem.* 73 (2008) 889-899.
- [119] W.F. DeGrado, C.M. Summa, V. Pavone, F. Nastri, A. Lombardi, *Annu. Rev. Biochem.* 68 (1999) 779-819.
- [120] C.A. Floudas, H.K. Fung, S.R. McAllister, M. Mönnigmann, R. Rajgaria, *Chem. Eng. Sci.* 61 (2006) 966-988.
- [121] G. Kiss, D. Röthlisberger, D. Baker, K.N. Houk, *Protein Sci.* 19 (2010) 1760-1773.
- [122] G.A. Jeffrey, W. Saenger, *Hydrogen Bonding in Biological Structures*, Springer-Verlag Berlin, Heidelberg: Berlin, 1991.
- [123] W.J. Song, M.S. McCormick, R.K. Behan, M.H. Sazinsky, W. Jiang, J. Lin, C. Krebs, S.J. Lippard, *J. Am. Chem. Soc.* 132 (2010) 13582-13585.
- [124] A.D. Bochevarov, J. Li, W.J. Song, R.A. Friesner, S.J. Lippard, *J. Am. Chem. Soc.* 133 (2011) 7384-7397.
- [125] E.I. Solomon, T.C. Brunold, M.I. Davis, J.N. Kemsley, S.-K. Lee, N. Lehnert, F. Neese, A.J. Skulan, Y.-S. Yang, J. Zhou, *Chem. Rev.* 100 (2000) 235-350.
- [126] R.A. Reynolds, III, W.R. Dunham, D. Coucouvanis, *Inorg. Chem.* 37 (1998) 1232-1241.
- [127] A.L. Gavrilova, B. Bosnich, *Chem. Rev.* 104 (2004) 349-384.
- [128] R.B. Hill, D.P. Raleigh, A. Lombardi, W.F. DeGrado, *Acc. Chem. Res.* 33 (2000) 745-754.

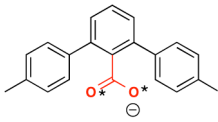
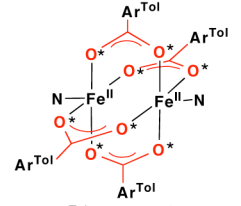
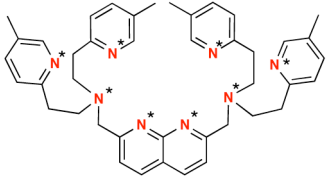
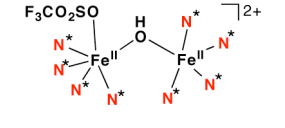
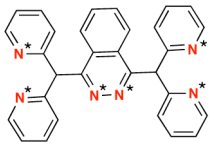
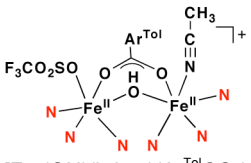
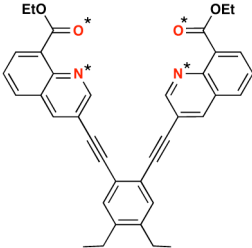
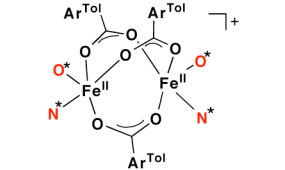
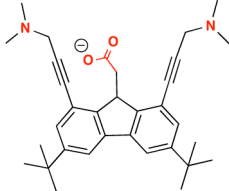
- [129] A. Lombardi, C.M. Summa, S. Geremia, L. Randaccio, V. Pavone, W.F. DeGrado, Proc. Natl. Acad. Sci. U.S.A. 97 (2000) 6298-6305.
- [130] I. Siewert, C. Limberg, Chem. Eur. J. 15 (2009) 10316-10328.
- [131] A. Stassinopoulos, J.P. Caradonna, J. Am. Chem. Soc. 112 (1990) 7071-7073.
- [132] M. Martinho, G. Xue, A.T. Fiedler, L. Que, Jr., E.L. Bominaar, E. Münck, J. Am. Chem. Soc. 131 (2009) 5823-5830.
- [133] G. Xue, D. Wang, R. De Hont, A.T. Fiedler, X. Shan, E. Münck, L. Que, Jr., Proc. Natl. Acad. Sci. U.S.A. 104 (2007) 20713-20718.
- [134] D. Wang, E.R. Farquhar, A. Stubna, E. Münck, L. Que, Jr., Nature Chem. 1 (2009) 145-150.
- [135] M.-H. Baik, B.F. Gherman, R.A. Friesner, S.J. Lippard, J. Am. Chem. Soc. 124 (2002) 14608-14615.
- [136] K.P. Jensen, C.B. Bell, III, M.D. Clay, E.I. Solomon, J. Am. Chem. Soc. 131 (2009) 12155-12171.
- [137] M. Costas, K. Chen, L. Que, Jr., Coord. Chem. Rev. 200-202 (2000) 517-544.
- [138] S. Mukerjee, A. Stassinopoulos, J.P. Caradonna, J. Am. Chem. Soc. 119 (1997) 8097-8098.

Table 1. Various Ligands Employed to Prepare Diiron Protein Model Complexes.

Ligand/ Example of Iron Complex ^a	Desirable Characteristics	Undesirable Characteristics	Reference No.
Mononucleating, Polydentate N-Heterocyclic Ligands			
 <p>TP⁻</p>	 <p>[Fe₂(O)(CH₃CO₂)₂(TP)₂] (1)</p>	<ul style="list-style-type: none"> • Forms stable tripodal chelate with iron • N-donors similar to histidine residues • Easy to synthesize 	<ul style="list-style-type: none"> • Capping unit restricts binding to the metal center • Does not enforce dinuclearity <p>37-39, 41</p>
 <p>BIPhMe</p>	 <p>[Fe₂(HCO₂)₄(BIPhMe)₂] (3)</p>	<ul style="list-style-type: none"> • Contains biomimetic imidazole groups • Bidentate chelate allows assembly of asymmetric diiron unit with open sites • Easy to synthesize 	<ul style="list-style-type: none"> • Does not enforce dinuclearity <p>42, 43</p>
Dicarboxylate Ligands			
 <p>MPDP²⁻</p>	 <p>[Fe₂(O)(MPDP)(BIPhMe)₂Cl₂] (6)</p>	<ul style="list-style-type: none"> • Enables assembly of [Fe^{III}₂O] units that could not be accessed using simple carboxylates 	<ul style="list-style-type: none"> • Does not enforce dinuclearity <p>44, 45</p>
 <p>XDK²⁻</p>	 <p>[Fe₂(XDK)(CyPhCO₂)₂(Py)₂] (9)</p>	<ul style="list-style-type: none"> • Supports a diiron core with open sites for substitution with external carboxylates and N-donor ligands • Maintains a dinuclear structure upon reaction with dioxygen 	<ul style="list-style-type: none"> • Endo positioning of carboxylates may be too geometrically restrictive • Does not prevent polynuclear aggregation <p>49-57</p>
 <p>Ph₄DBA²⁻</p>	 <p>[Fe₂(OH)(Ph₄DBA)(TMEDA)₂(CH₃CN)]⁺ (10)</p>	<ul style="list-style-type: none"> • Supports an {Fe₂(OH)} core with an open binding site for dioxygen • Stabilizes an oxygenated adduct to the diiron center 	<ul style="list-style-type: none"> • Does not prevent formation of tetranuclear complexes <p>60, 61</p>
 <p>PDK⁴⁻</p>	 <p>[Fe₃(PDK)(Lut)(Br)₂(HBr)] (12)</p>	<ul style="list-style-type: none"> • Provides both porphyrin and non-porphyrin binding sites 	<ul style="list-style-type: none"> • Does not prevent formation of polyiron clusters • Difficult to prepare in gram quantities <p>62-64</p>

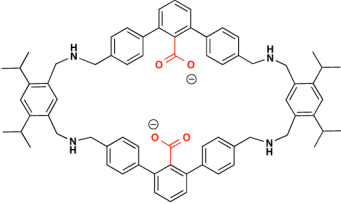
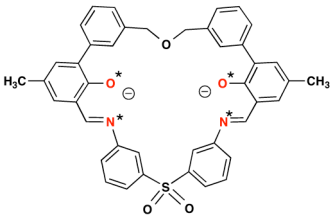
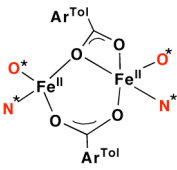
^aThe donor atoms highlighted in red and marked with an asterisk(*) in the iron complexes (second column) are derived from the donor groups, also shown with an asterisk, of the featured ligand (first column).

Table 1. (Continued)

Ligand/ Example of Iron Complex ^a	Desirable Characteristics	Undesirable Characteristics	Reference No.	
Terphenylcarboxylate Ligands				
 <p style="text-align: center;">$\text{Ar}^{\text{Tol}}\text{CO}_2^-$</p>	 <p style="text-align: center;">$[\text{Fe}_2(\text{Ar}^{\text{Tol}}\text{CO}_2)_4(4\text{-tBuPy})_2]$ (14A)</p>	<ul style="list-style-type: none"> • Forms diiron complexes in the presence of Fe(II) salts and an appropriate base • Stabilizes high-valent iron species • Easy to synthesize 	<ul style="list-style-type: none"> • The steric encumbrance of the 2,6-aryl groups restricts access to the diiron core • Does not prevent formation of polyiron species 	72-75, 77-78, 80-95
Dinucleating Polynitrogen Ligands				
 <p style="text-align: center;">BPEAN</p>	 <p style="text-align: center;">$[\text{Fe}_2(\text{OH})(\text{BPEAN})(\text{SO}_3\text{CF}_3)_2]^{2+}$ (24)</p>	<ul style="list-style-type: none"> • Contains a “masked carboxylate” to bridge two metal centers • Stabilizes diiron species in multiple oxidation states 	<ul style="list-style-type: none"> • Nitrogen-rich, rather than carboxylate-rich 	99-102
 <p style="text-align: center;">bdptz</p>	 <p style="text-align: center;">$[\text{Fe}_2(\text{OH})(\text{bdptz})(\text{Ar}^{\text{Tol}}\text{CO}_2)(\text{SO}_3\text{CF}_3)(\text{CH}_3\text{CN})]^{2+}$ (28)</p>	<ul style="list-style-type: none"> • Forms very stable bimetallic compounds 	<ul style="list-style-type: none"> • Nitrogen-rich, rather than carboxylate-rich 	103, 104
syn N-Donor Ligands				
 <p style="text-align: center;">$\text{Et}_2\text{BCQEB}^{\text{Et}}$ 1</p>	 <p style="text-align: center;">$[\text{Fe}_2(\text{Ar}^{\text{Tol}}\text{CO}_2)_3(\text{Et}_2\text{BCQEB}^{\text{Et}})]^{2+}$ (30)</p>	<ul style="list-style-type: none"> • Enforces the syn stereochemistry of nitrogen donors relative to the Fe–Fe vector • Accommodates binding of external carboxylates to the diiron core 	<ul style="list-style-type: none"> • Neutral oxygen donors, rather than anionic • Quinoline ester group does not sufficiently stabilize the iron centers 	105-110
 <p style="text-align: center;">DAFA⁻</p>	N.A.	<ul style="list-style-type: none"> • Contains a bridging carboxylate unit in addition to two adjacent amine groups 	<ul style="list-style-type: none"> • Not sufficiently pre-organized, could not metallate with iron • No clear advantage over $\text{Et}_2\text{BCQEB}^{\text{Et}}$ design 	111

^aThe donor atoms highlighted in red and marked with an asterisk(*) in the iron complexes (second column) are derived from the donor groups, also shown with an asterisk, of the featured ligand (first column). N.A. = not available.

Table 1. (Continued)

Ligand/ Example of Iron Complex ^a	Desirable Characteristics	Undesirable Characteristics	Reference No.
Macrocyclic Ligands			
 <p data-bbox="318 573 431 600" style="text-align: center;">$MAr^{Tol}CO_2^{2-}$</p>	N.A.	<ul style="list-style-type: none"> • May help control the nuclearity of the resulting iron complex 	115
 <p data-bbox="347 863 406 890" style="text-align: center;">PIM^{2-}</p>	 <p data-bbox="618 814 816 869" style="text-align: center;">$[Fe_2(Ar^{Tol}CO_2)_2(PIM)]$ (34)</p>	<ul style="list-style-type: none"> • Supports a carboxylate-bridged diiron(II) unit • Maintains a dinuclear core upon reaction with O_2 • Can be sterically tuned without obstructing access to the metal binding pocket. 	116

^aThe donor atoms highlighted in red and marked with an asterisk(*) in the iron complexes (second column) are derived from the donor groups, also shown with an asterisk, of the featured ligand (first column). N.A. = not available.

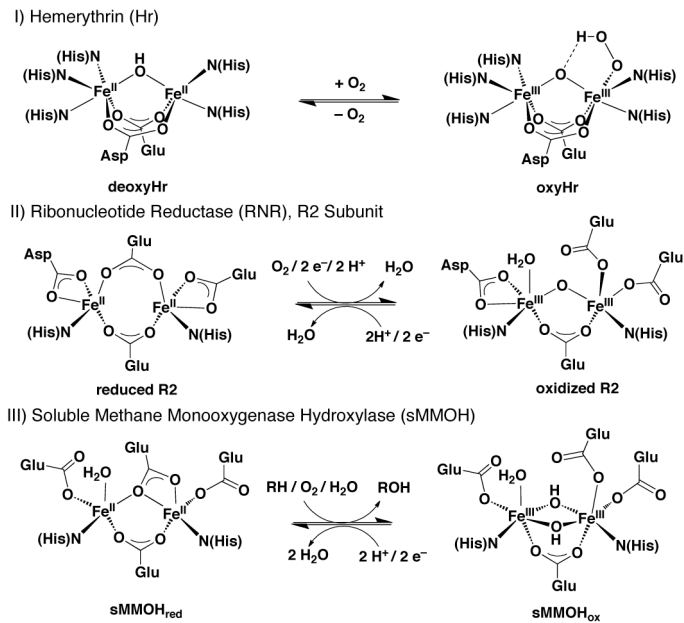
Scheme 1. Dioxygen reactivity of hemerythrin (Hr, top), ribonucleotide reductase (RNR, middle), and soluble methane monooxygenase hydroxylase (sMMOH, bottom). The active site structures of the proteins in various redox states are depicted.

Scheme 2. A proposed mechanism for the reaction of $[\text{Fe}^{\text{II}}_2(\mu\text{-Ar}^{\text{Tol}}\text{CO}_2)_4(4\text{-}^t\text{Bupy})_2]$ (**14A**) with O_2 [74, 75]. The actual structure of the diiron(III,IV) species **16** has not yet been determined.

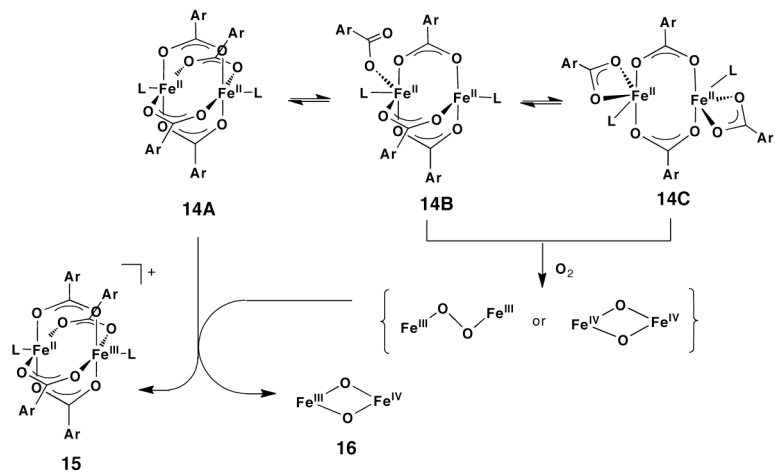
Scheme 3. A cartoon depiction of a diiron(II) model complex (**39**) containing a more sterically-hindering PIM^{2-} ligand, where the dark wedges represent a bulky organic substituent. Reaction of **39** with dioxygen may lead to a carboxylate shift and formation of a di(μ -hydroxo)diiron(III) product (**40**). The steric repulsion between the bulky PIM^{2-} substituents should prevent undesired formation of $[\text{Fe}^{\text{III}}_4(\mu\text{-OH})_6(\text{bulky PIM})_2(\text{RCO}_2)_2]$ (**41**) complexes.

Chart 1. Tethered substrates that could be successfully oxidized with O_2 when integrated into a diiron(II) terphenylcarboxylate complex. The starting substrate is depicted on top and the product isolated after oxygenation is shown directly below.

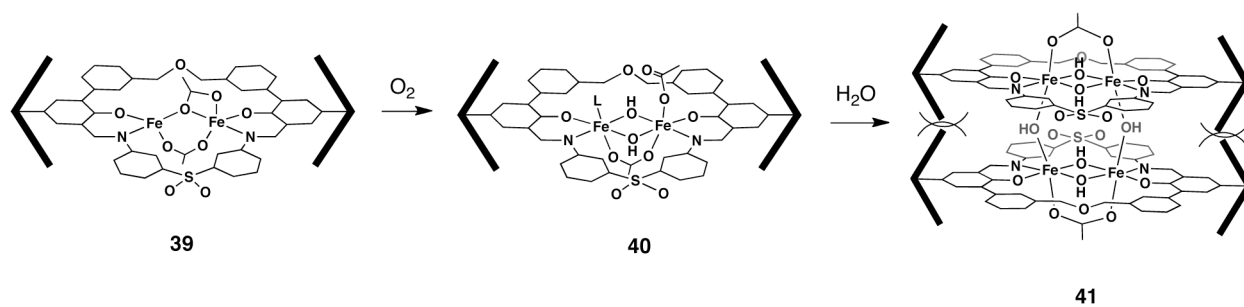
Chart 2. Examples of crystallographically characterized $[\text{Fe}^{\text{II}}_2(\text{syn } N\text{-donor})_2]$ species isolated from reaction of iron(II) salts and the corresponding syn *N*-donor ligand. Additional external carboxylate ligands were used in the preparation in some cases. PIC_2DET = bis(picolinic methyl ester)diethynyltriptycene [106]; Im_2DET = bis(*N*-methylimidazole)diethynyltriptycene [106]; $[\text{L}^{\text{Me,Ph}}]^{2-}$ = bis(phenyl(*p*-cresol)pyridyl)diethynylbenzene [110]; $\text{Ar}^{\text{Tol}}\text{CO}_2^-$ = 2,6-di(*p*-tolyl)benzoate.



Scheme 1.



Scheme 2.



Scheme 3.

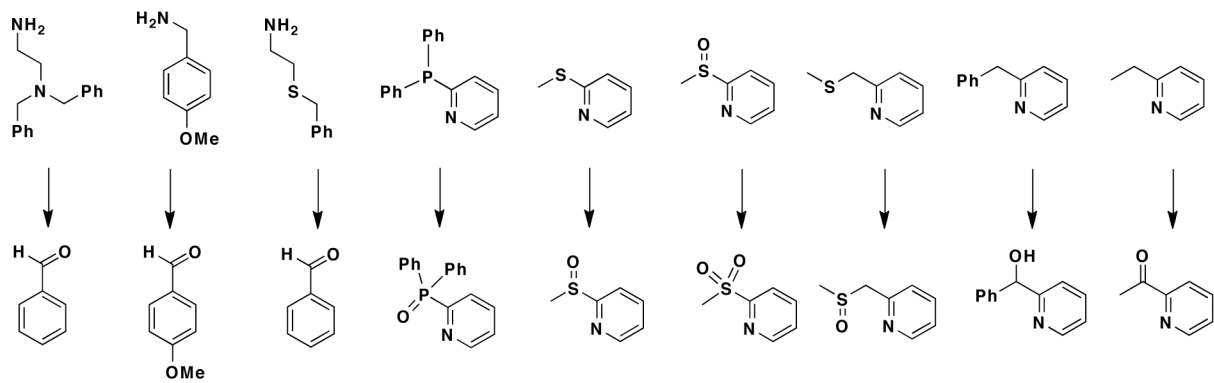
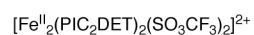
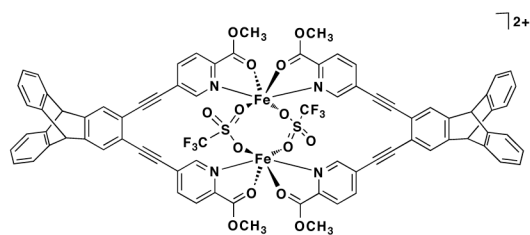
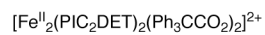
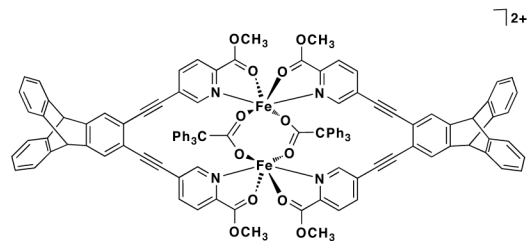


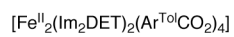
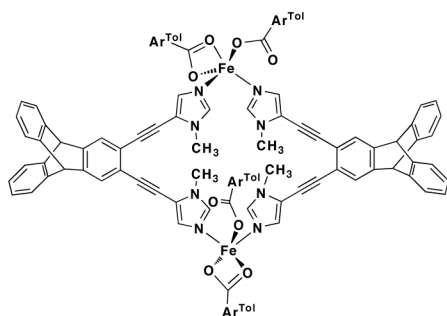
Chart 1.



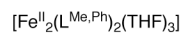
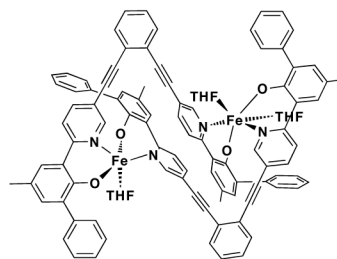
32A



32B

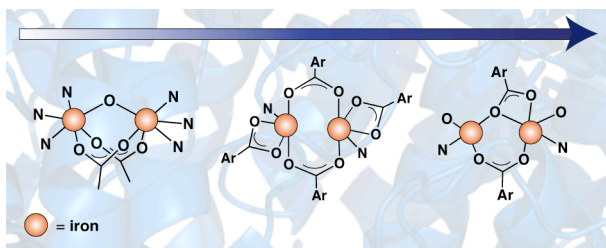


32C



32D

Chart 2.



Graphical Abstract